





## Article

# The CRATI Project: New Insights on the Consolidation of Salt Weathered Stone and the Case Study of San Domenico Church in Cosenza (South Calabria, Italy)

Michela Ricca <sup>1</sup>, Emilia Le Pera <sup>1</sup>, Maurizio Licchelli <sup>2,3</sup>, Andrea Macchia <sup>1,4</sup>,  
Marco Malagodi <sup>3,5</sup>, Luciana Randazzo <sup>1</sup>, Natalia Rovella <sup>1</sup>, Silvestro A. Ruffolo <sup>1</sup>,  
Maduka L. Weththimuni <sup>2</sup> and Mauro F. La Russa <sup>1,6,\*</sup>

<sup>1</sup> Department of Biology, Ecology and Earth Sciences, University of Calabria, 87036 Arcavacata di Rende (CS), Italy; michela.ricca@unical.it (M.R.); emilia.lepera@unical.it (E.L.P.); andrea-macchia@tiscali.it (A.M.); luciana.randazzo@unical.it (L.R.); natalia.rovella@unical.it (N.R.); silvio.ruffolo79@gmail.com (S.A.R.)

<sup>2</sup> Department of Chemistry, University of Pavia, 27100 Pavia, Italy; maurizio.licchelli@unipv.it (M.L.); madukalankani.weththimuni@unipv.it (M.L.W.)

<sup>3</sup> Arvedi Laboratory of Non-Invasive Diagnostics, University of Pavia, 26100 Cremona, Italy; marco.malagodi@unipv.it

<sup>4</sup> YOUTH in Conservation of Cultural Heritage, YOCOCU, 00175 Rome, Italy

<sup>5</sup> Department of Musicology and Cultural Heritage, University of Pavia, 26100 Cremona, Italy

<sup>6</sup> Institute of Atmospheric Sciences and Climate, National Research Council, 40129 Bologna, Italy

\* Correspondence: mlarussa@unical.it

Received: 16 April 2019; Accepted: 20 May 2019; Published: 22 May 2019



**Abstract:** This paper presents the results of a laboratory experimentation carried out on stone materials in the framework of the CRATI project (Knowledge and Restoration through Advanced Integrated Technologies) aimed at testing new products with consolidating properties by means of an integrated methodological approach. After the preliminary characterization of stone materials collected in the pilot site, the second stage of the activities within the project were focused on the formulation and testing of products for the conservation of the same materials against decay, especially salt crystallization, one of the most aggressive and common degrading processes. The San Domenico Church, located in the old town of Cosenza (Calabria, Southern Italy) has been chosen as the pilot site and for the in situ tests. Several specimens with the same features of the stone materials used in San Domenico church were collected from a historical quarry near the city of Cosenza. These specimens were treated and then artificially degraded by salt crystallization tests in order to evaluate their susceptibility to weathering intensity. Three different consolidating products were used; respectively, two commercial and another one formulated in laboratory: (a) a suspension of nanosilica (Nano Estel<sup>®</sup>); (b) a suspension of nanolime (CaLoSiL<sup>®</sup>), and (c) a suspension of nano calcium-hydroxide dispersed in isopropyl alcohol and then mixed with diammonium hydrogen phosphate. A systematic approach, including minero-petrographic, geochemical and physico-mechanical techniques, was applied to evaluate (a) the nature and main features of materials; (b) the efficacy of consolidating treatments, and (c) the resistance of treated stone to the salt crystallization processes. The tested products demonstrated a significant efficiency to consolidate and protect stone material samples, enhancing their resistance to salt crystallization. Thus, such a case history may be useful in order to plan appropriate restoration interventions that consider the interactions between the building stone and the protective/consolidating product.

**Keywords:** biocalcarenites; stone decay; soluble salt crystallization; consolidation treatments; hydroxyapatite

## 1. Introduction and Historical Setting

The conservation of weathered stones is an important topic in the field of cultural heritage and restoration activity, such that the correct choice of conservation strategy represents an essential objective for scientists working in this research area, to be applied to, and evaluate on a case by case basis.

Consolidation treatments aim to prevent stone decay, decohesion phenomena and weathering forms. Specifically, a consolidant product is used to improve the cohesion of weathered stones when serious decay patterns and in-depth cohesion loss are present in order to increase the mechanical strength of the rock [1–4]. In addition, the application of suitable products leads to a reduction of the stone's susceptibility to various decay phenomena, and especially to soluble salt crystallization decay [5]. The latter is one of the most dangerous weathering agents in porous building materials that limit its durability, particularly in limestone [6–10]. For this reason, the first step is to understand deeply this degradation process, in order to prevent or limit the damage. Secondly the experimentation of innovative consolidation products is required to identify those most appropriate, considering their compatibility with both the environment and the materials.

The aim of this study is to assess the behaviour of consolidated “Mendicino stone” (also known as “San Lucido stone”) to salt crystallization weathering, a calcarenite largely employed for vernacular and monumental architecture in Cosenza Province [11–13], such as the San Domenico Church (Cosenza, Italy), the pilot site of this research.

This historical monument is located in the old town of Cosenza (Calabria, southern Italy) and belongs to a Dominican complex dating back to the fifteenth century. Geographically it is placed to the left-side of the Crati river, near its confluence with the Busento river (Figure 1). This complex represents one of the most important historical buildings of the city, with an initial Gothic architectural influence that has undergone stylistic changes over time, especially during the Renaissance and Baroque periods. The church, as the central unit of the whole complex, reflects the typical features of the mendicant orders with a single rectangular room covered by a wooden ceiling and a quadrangular choir overhung by a ribbed vault [14,15]. The façade is composed of three parts: (a) the pediment (no longer visible) with the tympanum, (b) the rose window and (c) the prothyrum with a sixth-acute arch and denticular cornice. The main portal, which, along with the prothyrum was selected as the case study (Figure 2), is made up of calcarenite and characterised by a sixth-acute arch composed of large trapezoidal ashlars, with the exception of the triangular-shaped ashlar-key, and springers with a rectangular section. The arch is framed by a geometrical molding, alternating with shaped bands of rod, strip and inverted throat [14,15].

After the preliminary characterization of stone materials collected in the pilot site through minero-petrographic and geochemical techniques, the second phase of activity was devoted to the formulation and testing of products for the church conservation. For this purpose, several specimens from a historical quarry near the city of Cosenza (i.e., San Lucido) were collected. The outcrops of this building material are situated in an area including the southern part of the Coastal Thyrrenian Range, from San Lucido to Domanico, and the right side of the Crati River, from Laurignano to Altiglia villages [16–19]. The quarry has been active since the 1950s in the northern area of San Lucido, and three newer quarries are still active [20]. Natural lithotypes, then analysed for this research, have been sampled in one of these three quarries. In particular, samples were mesoscopically characterized, consolidated and artificially weathered by salt crystallization tests. To evaluate their consolidating effectiveness, a systematic approach, including colorimetric tests (CT), peeling test or the so-called “scotch tape test” (STT) and point load test (PLT), was used.



**Figure 1.** (a) Cosenza city map: red circle indicates the San Domenico church; (b) panoramic view of the San Domenico church.



**Figure 2.** Portal of San Domenico Church (Cosenza, Italy) and details of the sampled areas.

## 2. Materials and Analytical Methods

### 2.1. Sampling and Macroscopic Characterization

An exhaustive sampling of the San Domenico building stones was performed, with the assistance of the Superintendence of Archaeology, Fine Arts and Landscape for the Provinces of Catanzaro, Cosenza and Crotona, who retrieved small samples in different representative areas of the pilot site (Figure 1).

Specifically, the prothyrum and the main portal, both attributable to the original building of the Dominican complex, were selected as cases study. Before sampling, a preliminary survey aimed to verify the state of preservation of the portal was carried out. In particular, the main detected forms of degradation are characterised by surface deposits (accumulation of dust, soil, etc. due to outdoor exposure), black crusts, erosion (mainly diffused in the lower part of the portal and in the areas concerned with black crusts' presence), chromatic alteration (distributed over large areas), loss of material (mainly diffused in the lower part of the portal) and biological patinas.

After mapping decay forms, eleven fragments were sampled and then studied with different and complementary techniques. A list of analysed specimens, along with a brief macroscopic description and techniques used to study, is summarized in Table 1.

**Table 1.** Macroscopic features of investigated samples together with the sampling areas according to Figure 1 and employed techniques on each sample. POM = polarizing microscope; XRD = X ray diffraction; FT-IR = Fourier transform infrared spectroscopy; EMPA-EDS = electron microprobe analysis.

Historical Stone Samples			
ID Sample	Description	Sampling Point	Employed Techniques
SD1	Fragment of calcarenite, no macroscopic evidence of superficial alteration forms.	Prothyrum. Base of the cluster pillar, right side.	POM, XRD
SD2	Fragment of calcarenite, no macroscopic evidence of superficial alteration forms.	Prothyrum. Base of the cluster pillar, right side.	POM, XRD
SD3	Fragment of calcarenite, no macroscopic evidence of superficial alteration forms.	Prothyrum. First ashlar on the lower part of the cluster pillar, right side.	POM, XRD
SD4	Fragment of calcarenite, macroscopic evidence of a greyish superficial layer.	Prothyrum. Base of the cluster pillar, left side.	POM, XRD, FT-IR, EMPA-EDS
SD6	Fragment of calcarenite, no macroscopic evidence of superficial alteration forms.	Prothyrum. Along the intersection between the left cluster pillar and the lateral front.	POM, XRD
SD8	Fragment of calcarenite, macroscopic evidence of a blackish superficial layer.	Main portal. Base of the cluster pillar, left side.	POM, XRD, FT-IR
SD9	Fragment of calcarenite, macroscopic evidence of a blackish superficial layer.	Main portal. Base of the cluster pillar, left side.	POM, XRD, FT-IR, EMPA-EDS
SD10	Fragment of calcarenite, macroscopic evidence of a greyish superficial layer.	Main portal. Cluster pillar, left side.	POM, XRD, FT-IR
SD11	Fragment of calcarenite, macroscopic evidence of a greyish superficial layer.	Main portal. Pier, left side.	POM, XRD, FT-IR
SD12	Fragment of calcarenite, macroscopic evidence of a blackish superficial layer.	Main portal. Cluster pillar, right side.	POM, XRD, FT-IR
SD13	Fragment of calcarenite, macroscopic evidence of a blackish superficial layer.	Main portal. Base of the cluster pillar, right side.	POM, XRD, FT-IR

## 2.2. Diagnostic Analysis

Diagnostic investigations on the selected stones samples were carried out in two main stages: (a) the mineralogical-petrographic characterization of lithotypes and (b) the evaluation of damage and weathering forms. Specifically, the analytical techniques applied for a complete study of the samples include:

Polarising optical microscopy (POM) was performed on thin sectioned lithotypes samples and stratigraphic sections. Observations were performed using a Zeiss AxioLab microscope (Oberkochen, Germany) equipped with a digital camera to capture images.

X-ray diffraction analysis (XRD) was used to identify the constituent mineralogical phases, separating the altered layer from stone. Analyses were performed on a D8 Advance Bruker



diffractometer (Billerica, MA, USA) with Cu K $\alpha$  radiation, using the following operative conditions: step-size of 0.02° 2 $\theta$ , step time of 2s/step and an analytical range of 3°–65°.

Fourier Transform Infrared Spectroscopy (FT-IR) was used to characterize the superficial layers of the samples. The spectrophotometer used is a Perkin Elmer Spectrum 100 (Waltham, MA, USA), equipped with an attenuated total reflectance (ATR) accessory. Infrared spectra were recorded in ATR mode, in the range of 500–4000 cm<sup>−1</sup> at a resolution of 4 cm<sup>−1</sup>.

Electron microprobe analysis (EMPA) was carried out by a JEOL JXA 8230 equipment (Tokyo, Japan), coupled with a spectrometer EDS–JEOL EX-94310FaL1Q, silicon drift type, to examine the microstructures and the major element compositions of the altered superficial layers. The measurements were performed on polished thin sections coated with a thin and highly conductive film (graphite).

### 2.3. Laboratory Tests

Laboratory tests were performed on calcarenite samples on the basis of the main degradation products revealed by diagnostic analyses and taking into account the need to consolidate the stone. Natural lithotypes from a historical quarry near the city of Cosenza (i.e., San Lucido) were collected and used for the laboratory tests. The samples were first treated by applying three different consolidating products and then artificially degraded by salt crystallization tests in order to evaluate their susceptibility to weathering. Concerning products, two commercial and another formulated in the laboratory were experimented: (a) a suspension of nanosilica (Nano Estel® (CTS srl, Vicenza, Italy)); (b) a suspension of nanolime (CaLoSiL® (Bresciani srl, Milano, Italy)), and (c) a suspension of nano calcium-hydroxide dispersed in isopropyl alcohol and then mixed with diammonium hydrogen phosphate. Ca(OH)<sub>2</sub> nanoparticles were synthesized in the laboratory by a standard method [21]. Then, Ca(OH)<sub>2</sub> propan-2-ol dispersion (5 g L<sup>−1</sup>) was prepared and kept under nitrogen atmosphere in order to eliminate the carbonation process. After that, 5% (w/w) of (NH<sub>4</sub>)<sub>2</sub>HPO<sub>4</sub> (DAHP) solution was prepared.

Each formulation has been applied on stone specimens (5 cm × 5 cm × 2 cm) by brushing in two different amounts and treating half of the total area of the specimen (Table 2). In particular, the application of the product synthesized in the laboratory took place in two steps: (a) 5 g L<sup>−1</sup> Ca(OH)<sub>2</sub> nanoparticles were applied on stone samples until the surfaces were getting saturation; (b) 24 h later the application of nanoparticles, 5% (w/w) diammonium hydrogen phosphate was also applied to those surfaces until they were getting saturation. In all steps of the laboratory experimentation, untreated samples were used to make a comparison with treated specimens. Both before and after treatment, some physical and mechanical properties were measured by means of the following techniques:

Colorimetric tests (CT) were carried out using a CM-2600d Konica Minolta spectrophotometer (Tokyo, Japan), to assess chromatic variations according to [22]. Chromatic values are expressed in the CIE L\*a\*b\* space, where L\* is the lightness/darkness coordinate, a\* the red/green coordinate (+a\* indicating red and −a\* green) and b\* the yellow/blue coordinate (+b\* indicating yellow and −b\* blue). This analysis was aimed to assess the colour variation induced by the treatment.

The Scotch tape test (STT) is defined as a method to quantify the adhesion of a surface or a near to-surface layer to a substrate. According to [23], a pressure-sensitive tape was applied to the investigated area and then pulled off. The weight of material detached from the surface after peeling off the tape was measured. The test was repeated five times on the same area. It is generally assumed that this amount reflects the cohesion characteristics of the substrate. Therefore, the SST allowed to evaluate the surface degradation or consolidation effects after restoration procedures. Measurements were performed on three samples for each treatment.

A point load test (PLT) provided a strength assessment of unaltered and treated samples. According to [24], measurements have been carried out on the sample through the application of a pressure through a pair of truncated, conical platens. Measurements were performed on three samples for each treatment in order to calculate the average value. The load was increased up to sample failure, and the results are expressed as the failure load (MPa).

Lastly, after the consolidation of the stones and an evaluation of the formulation's properties, the salt crystallization test was carried out on untreated and treated specimens (three for each treatment) in order to establish the resistance of materials to weathering [6,7]. The procedure followed for salt crystallization is that described in the existing standard [25], modified according to [7]. More specifically, specimens underwent several crystallization cycles (15) consisting of: (a) 2 h of immersion in a supersaturated solution of sodium sulfate (14% *w/w* at 20 °C) for 10% of their height; (b) 8 h of drying in an oven at 45 °C, and (c) 16 h of cooling at room temperature. The weight of each test sample was measured before the crystallization test and after each cycle; the resulting weight loss was determined.

The workflow of the whole laboratory experimentation reporting the specimens list along with details on formulations and used methods is summarized in Table 2 and Figure 3. The experimentation consists of several phases: (a) specimen consolidation, (b) characterization of the formulations after application on the specimens, (c) salt weathering test on untreated and treated specimens to evaluate resistance to salt crystallization.

**Table 2.** List of specimens that underwent the three different phases of experimentation and details about products and methods used.

Sample Group ID.	Products/Formulations	Experimentation on Specimens				
		I Step	II Step		III Step	
		Preliminary Characterization Tests	Consolidant Treatment (g/cm <sup>2</sup> )	Consolidation Performance Tests	Salt Weathering (cycles)	Consolidation Performance Tests
CNLa	CaLoSiL <sup>®</sup>	Colorimetric Test, Scotch Tape Test, Point Load Test	0.36	Colorimetric Test, Scotch Tape Test, Point Load Test	15	Macroscopic evaluation of the damage and Point Load Test
CNLb	CaLoSiL <sup>®</sup>		0.18		15	
CNSa	Nano Estel <sup>®</sup>		0.32		15	
CNSb	Nano Estel <sup>®</sup>		0.16		15	
DAHPa	Mixture of Ca(OH) <sub>2</sub> and diammonium hydrogen phosphate		0.32		15	
DAHPb	Mixture of Ca(OH) <sub>2</sub> and diammonium hydrogen phosphate		0.16		15	
U	Untreated		–		15	

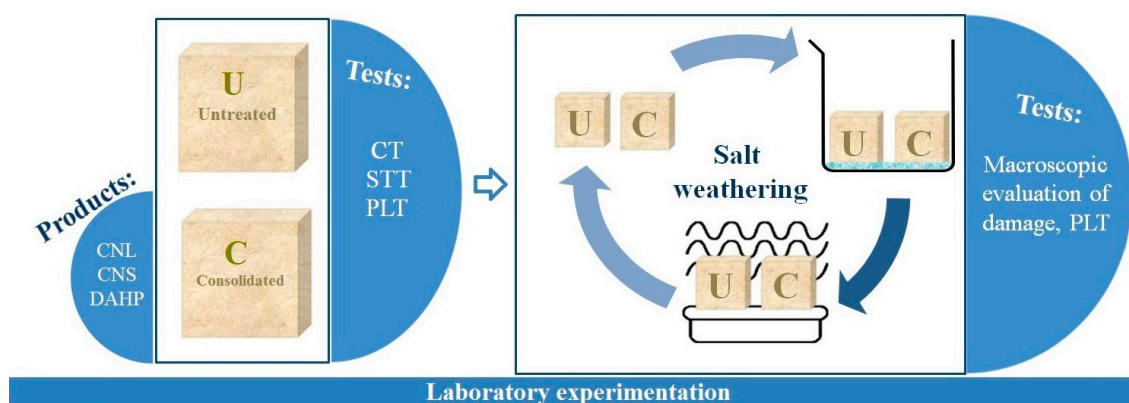


**Figure 3.** Scheme illustrating the experimentation workflow.

### 3. Results and Discussion

#### 3.1. Characterization of Stone Materials & Alteration Forms

##### 3.1.1. Polarising Optical Microscopy and X-ray Diffraction Analysis

Petrographic observations of the thin sections under optical microscope reveal that samples show similar compositional features. Specifically, they can be classified as biomicrites or packstone/grainstone (Figure 4A,B) [26,27] with the exception of the samples SD11 and SD12 which are biosparites (Figure 4C,D) and SD1 showing biosparitic/micritic properties. The framework components are bioclasts dominated by fragments of molluscan shells, bryozoans, foraminifera and echinoderms 1–2 mm in size. The most abundant accessory clasts are mainly siliciclastic and they are monocrystalline quartz, biotite, muscovite, K-feldspars, plagioclase and chlorite with grains ranging from 0.1 to 0.2 mm in size. Rarely, plutonic and metamorphic rock fragments occur, and the micritic matrix is not well represented within these samples. Cementations of these rocks include, on the basis of crystal morphology, small prismatic calcite cement and locally developed meniscus cement at grain contacts. Grain size distribution is quite heterogeneous, and it is composed of at least by two secondary modes and one principal mode that fall into the coarse-grained sand (microfossils). All samples show predominantly intergranular macroporosity with cavities demonstrating a variable and irregular shape, ranged in size from 0.2 to 5 mm.

A brownish and superficial layer up to 800 µm thick is often present on the substrate. The level is related to the alteration forms macroscopically observed, with variable colours, morphologies and thicknesses. Superficial layers appear, many irregularly shaped, constituted by microcrystalline gypsum with sporadic grains of calcite (from the substrate) and carbonaceous particles.

Deterioration layers that developed on biomicrites or packstone/grainstone show variable thickness and different degree of adherence to the substrate. In particular, the adherence is very weak, especially in those areas where subefflorescences made of soluble/hygroscopic salts are present. Furthermore, the morphology of black crusts on these surfaces follows approximately the profile of the underlying building material with episodic deeper penetrations of the alteration products along pore walls in the stone.

On substrates composed of biosparites, black crusts seem to grow homogeneously with a lesser thickness showing also a stronger adherence to the substrate.

As expected, biosparite rocks are definitely less sensitive than the biomicrites to the capillary rise of aqueous solutions (and consequently to damage from salt crystallization) because of their overall structural and textural features.

Insofar as the mineralogical phases are concerned, contents obtained by XRD, analyses confirmed a previous investigation to reveal that samples display a very similar mineralogical composition where calcite and quartz are the most representative phases characterizing the stone substrate, followed by accessory minerals such as feldspars, plagioclase, micas, chlorites, iron-oxides and clay minerals. Dolomite was also detected only in sample SD13. A contribution of the alteration is remarkable in almost of all the samples probably due to the difficulty encountered in perfectly separating the superficial altered layers from the stone substrate during sample preparation; in this regard gypsum and weddellite were detected. Table 3 reports in more detail the mineralogical phases of each sample detected by XRD.



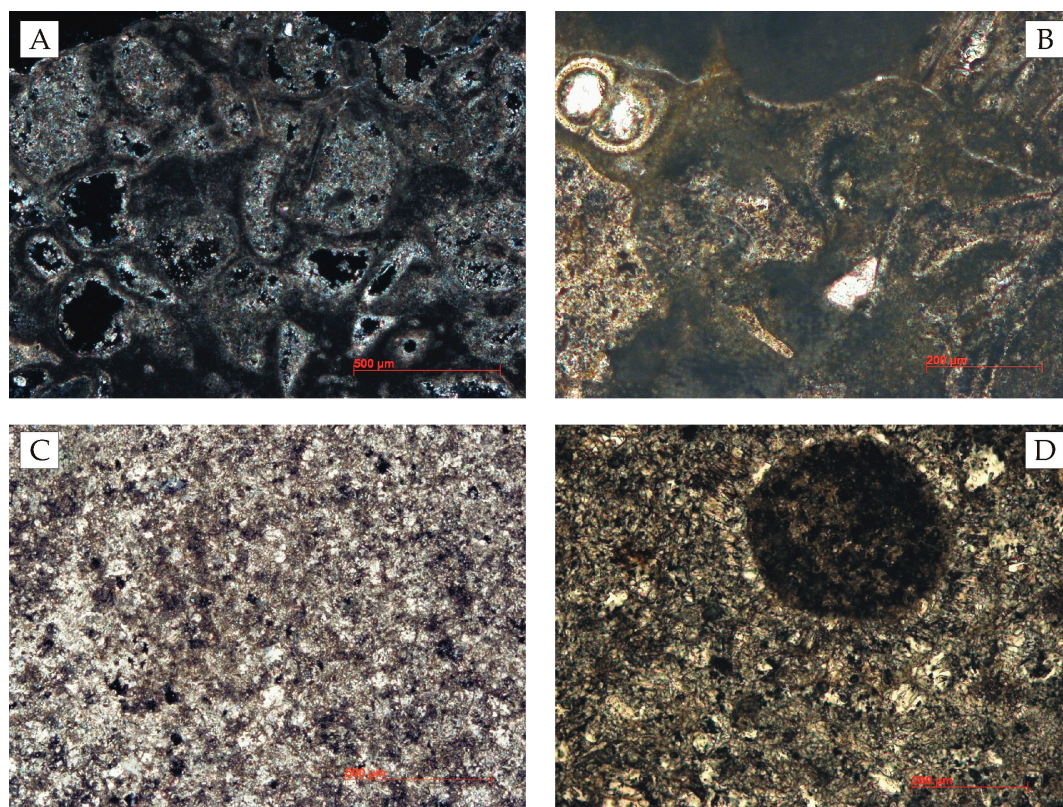


**Figure 4.** Representative photomicrographs by POM showing some textural features of biomicrites samples (A,B) and biosparites (C,D).

**Table 3.** Main mineralogical phases of investigated samples as obtained by XRD. Notes: Cal = calcite; Dol = dolomite; Qtz = quartz; Fds = feldspars; Pl = plagioclase; Gy = gypsum; Mic = micas; Chl = chlorite; Clay min. = clay minerals. Wed = weddellite; Fe.ox = iron oxides; ++++ = very abundant; +++ = abundant, ++ = moderate; + = scarce; (-) = absent.

Mineralogical Phases by XRD											
Sample	Cal	Dol	Fds	Mic	Chl	Pl	Qtz	Clay min.	Fe-ox	Gy	Wed
SD1	++++	(-)	(-)	++	+	(-)	++	(-)	+	(-)	(-)
SD2	++++	(-)	(-)	(-)	(-)	+	++	(-)	(-)	(-)	(-)
SD3	++++	(-)	(-)	++	(-)	+	++	(-)	+	(-)	(-)
SD4	++++	(-)	(-)	(-)	(-)	(-)	++	+	+	+	(-)
SD6	++++	(-)	+	+	(-)	+	++	(-)	+	(-)	(-)
SD8	++++	(-)	+	++	(-)	+	++	(-)	+	+	+
SD9	++++	(-)	(-)	++	(-)	(-)	++	(-)	(-)	+	(-)
SD10	++++	(-)	++	+	(-)	(-)	++	(-)	(-)	+	(-)
SD11	++++	(-)	(-)	(-)	(-)	(-)	+	(-)	(-)	+	(-)
SD12	++++	(-)	(-)	(-)	(-)	(-)	+	(-)	(-)	+	+
SD13	++++	+++	+	+	(-)	+	++	(-)	+	+	+

### 3.1.2. Fourier Transform Infrared Spectroscopy

Fourier transform infrared spectroscopy (FT-IR) was performed on samples showing macroscopic alteration forms (Table 1) in order to identify their nature and also to better validate the results obtained by means of POM and XRD.

Spectra from the samples SD4, SD9, SD10 and SD12 revealed a variable amount of gypsum ( $\text{CaSO}_4 \cdot 2\text{H}_2\text{O}$ ), showing the typical vibrational bands centred at 1109, 669, and  $596 \text{ cm}^{-1}$  as well as the



stretching vibrations of calcite ( $\text{CaCO}_3$ ), peaked at 1409, 875, and  $711\text{ cm}^{-1}$  [28] and quartz peaked at 1094 and  $457\text{ cm}^{-1}$ .

Calcite and quartz occur due to substrate, while the presence of gypsum can represent a degradation product. In fact, if calcium carbonate is attacked by sulphuric acid generated by the sulphur compounds in the polluted atmosphere, it is transformed into gypsum [29–34]. Spectra of the samples SD8, SD11 and SD13 exhibit all the previous bands; and in addition, those related to the presence of the characteristic bands of weddellite (calcium oxalate) peaked at around 1643, 1330 and  $783\text{ cm}^{-1}$ . The presence of this mineral is indicative of an alteration product [30,31,35,36]. Representative IR spectra are shown in Figure 5.

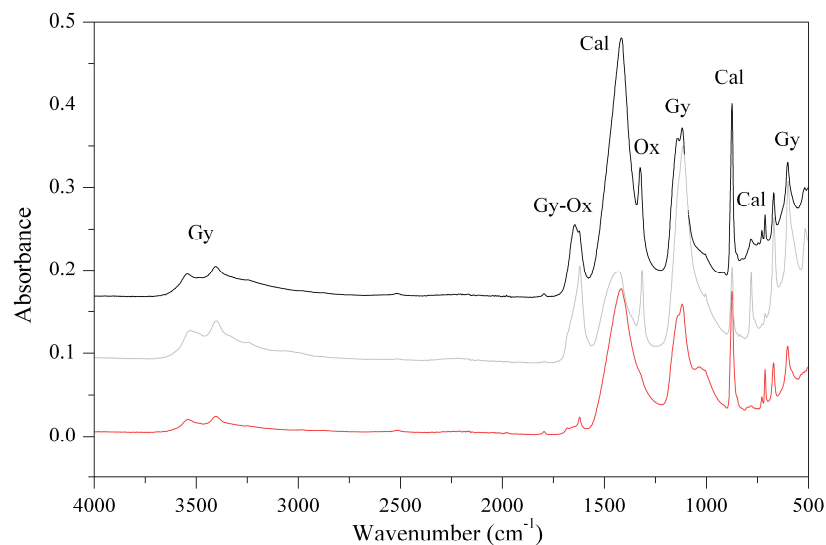


**Figure 5.** Representative FTIR spectra of some samples showing superficial alteration forms.

### 3.1.3. EMPA-EDS Analysis

The EMPA-EDS analysis was conducted on fragments showing stratified superficial level of alteration under optical microscope, respectively sample SD4 and SD9.

Investigation proved to be crucial, confirming stratigraphy supposed by means of POM observations. Both samples show a multi-layered superficial patina (2 levels) with thicknesses ranging between 400 and  $800\text{ }\mu\text{m}$ , for sample SD4, and varying from 30 to  $50\text{ }\mu\text{m}$  in SD9. In such samples the alteration adheres perfectly to the underlying rock and in some portions of the section it seems to penetrate inside the substrate, producing decohesion phenomena (Figure 6).

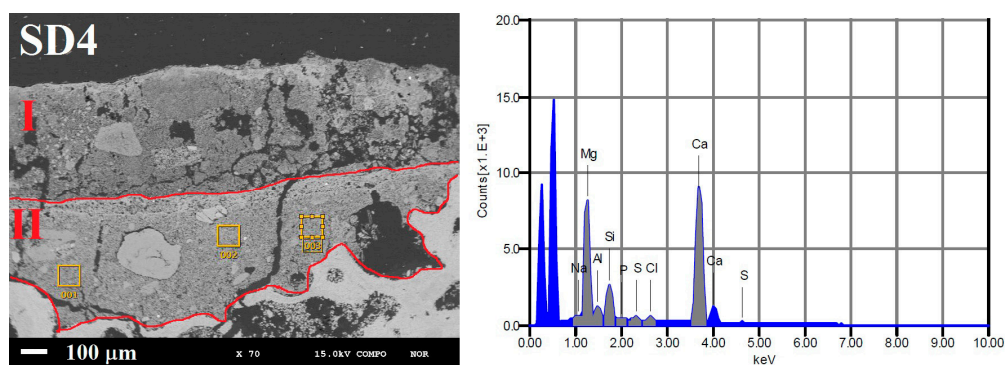


**Figure 6.** EMPA-EDS image of sample SD4 showing morphological features of multi-layered superficial patina (I and II layer) and some analysed areas (squared areas in II layer) by EDS.

From a chemical point of view, the EDS analyses reveal the similar composition in both layers, both for SD4 and SD9. In particular, the peaks of S and Ca can be attributable to gypsum, as characteristic component of the black crusts. On the contrary, the detection of other chemical elements such as Mg, Al, Si, Na, Cl could be related to the accessory mineralogical phases in the stone substrate and to the soluble salt crystallization (Figure 5). Five measurements were performed for each investigated sample and the average value was considered as representative of the chemical composition.

### 3.2. Laboratory Tests

For the laboratory experimentation, specimens were collected from the “San Lucido” quarry near the city of Cosenza, this stone is a widely studied material, the petrophysical properties of which are well known [16–20]. Stone samples were cut in sizes  $5\text{ cm} \times 5\text{ cm} \times 2\text{ cm}$ , cleaned and kept inside the oven at  $60\text{ }^{\circ}\text{C}$  for some days until they reached the constant weight (according to [37]).

#### 3.2.1. Colorimetric Tests (CT)

Chromatic variations have been calculated to assess the difference in colour between treated and untreated samples, in accordance with [22]. Results about colorimetric tests suggest that the colour change ( $\Delta E$ ) is generally around 3–4 for all products and can be considered acceptable [38].

#### 3.2.2. Scotch Tape Test (SST)

The Scotch tape test (SST) was performed to provide information on the superficial cohesion of stone in order to investigate better the mechanical features of treated samples and to correlate them with those untreated. The results are reported in Figure 7. Treated specimens show a decrease in released material compared to untreated specimens, achieving an improvement in their superficial cohesion. Also, specimens treated with greater quantities of product give a better result. In more detail, a greater efficacy in terms of increased cohesion properties was observed in the samples treated with a mixture of nano calcium-hydroxide and diammonium hydrogen phosphate.

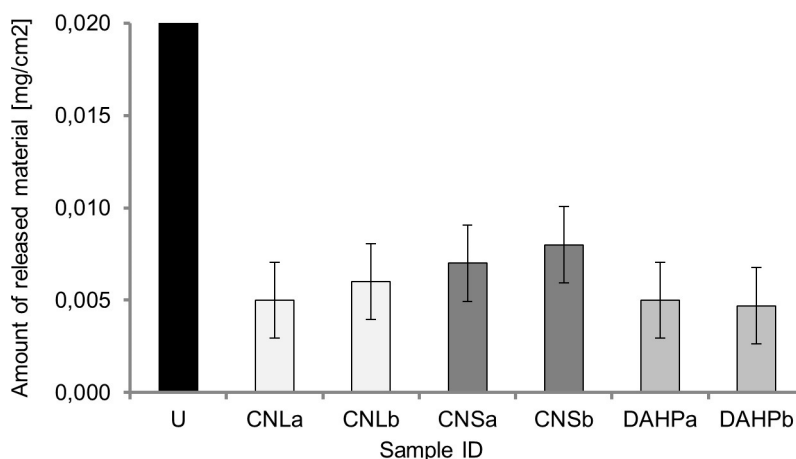


Figure 7. Scotch tape test on untreated and treated specimens.

#### 3.2.3. Salt Weathering and Consolidation Performance Tests by Point Load Test (PLT)

The salt crystallization test was carried out by partial immersion [7] on the basis of that standardized [25], but it is not considered to be the only one for the characterization of stone.

After just 24 h, saline solution had migrated through untreated calcarenite specimens as efflorescence. On the contrary, the consolidated samples showed efflorescence around the V-VI cycle. It depends on the evaporation speed of the solution at the stone surface that may have been conditioned by consolidant products [39].

During the various cycles, the samples are affected by increases and losses in weight up to the 10th–12th cycle, then increasing until the 15th cycle. In fact, the location of salt crystallization depends on the flow of the water and the permeability of the substrate, which allows the salt to move. Therefore, the crystallization of salt crystals is generally accompanied by an increase in volume, which produces internal stresses [40,41]. While the liquid phase allows salt to be transported, the evaporation, which can occur outside (efflorescence) or inside the material (subefflorescence), enables it to crystallize [5].

At the 15th cycles specimens suffered just rounding and loss of very small fragments, mainly at the edges. None of the samples suffered a break (Figure 8). Based on the results, and in accordance with [5], weight variations could be due to both the development of efflorescence and subefflorescence, and to the loss of material, although minimal, observed along the edges of the samples.

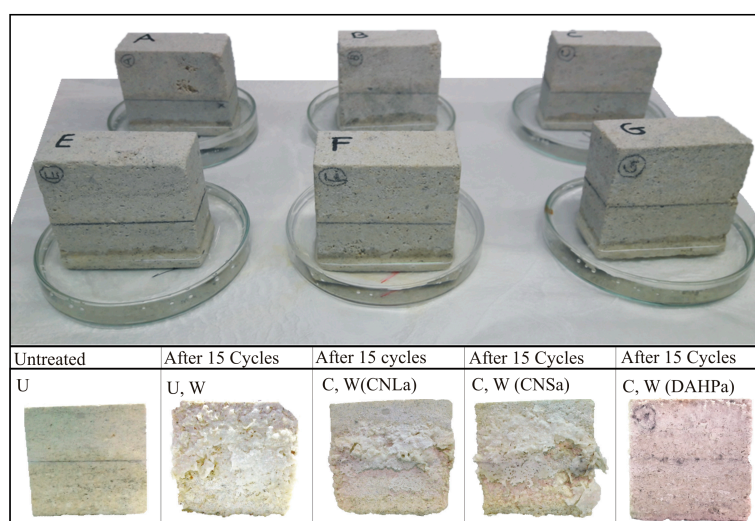


**Figure 8.** Salt weathering of some representative “San Lucido” stone specimens. Note: U, untreated; C, consolidated; W, weathered; CNL, CaLoSiL®; CNS, Nano Estel®; DAHP, Mixture of  $\text{Ca}(\text{OH})_2$  and diammonium hydrogen phosphate.

Considering the weights at each cycle and removing the efflorescence from each sample, the contribution of the subefflorescence was then evaluated. This occurs because, the longer the saline solution remains within the porous media, the worse the damage can be produced [42,43]. Figure 9 shows the increase in weight (%) that the specimens have undergone up to the 15th cycle, emphasizing the contribution made by the efflorescence compared to that made by the sub-efflorescence.

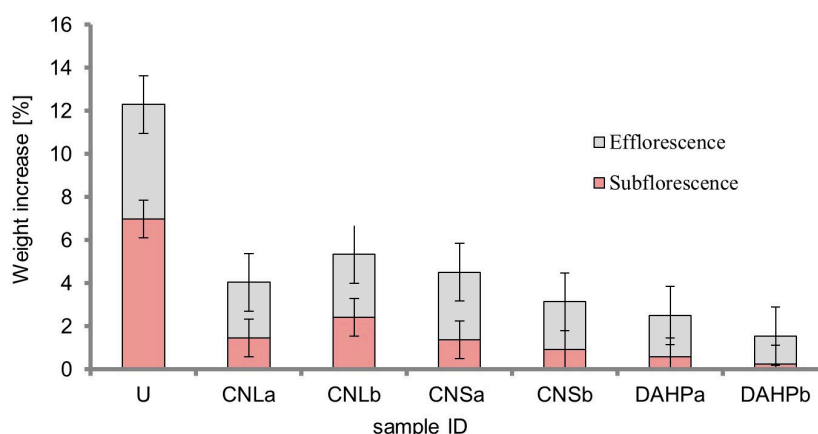


**Figure 9.** Weight increase (%) after salt crystallization test with evidence of the contribution of efflorescence and subefflorescence.

The difference between the consolidated and untreated samples is remarkable, both in terms of weight variations (at the end of the 15th cycle) as well as the growth of efflorescence and sub-efflorescence. These differences suggest that nano calcium-hydroxide mixed with diammonium hydrogen phosphate give a better response against salt crystallization decay process.

The point load test (PL) provides an indication of the stone strength and could be considered complementary to the peeling test measurement.

Figure 10 reports the failure load values for analysed samples. Tests were carried out on untreated, consolidated and salt-weathered specimens (after 15 cycles). The unaltered material (U) (Figure 10a) reaches a failure pressure slightly higher than 70 bar, while consolidated specimens a pressure ranging from about 90 to 95 bar, suggesting an increase of the material strength after the consolidating treatment. As for the same test, performed after 15 cycles of salt crystallization (Figure 10b), results show that weathered stones have a failure pressure respectively of: 40–45 bar for specimens treated with nanosilica (i.e., CNS, Nano Estel<sup>®</sup>), 70–72 bar for specimens treated with nanolime (i.e., CNL, CaLoSiL<sup>®</sup>) and 72–75 bar for those treated with a mixture of nano calcium-hydroxide mixed with diammonium hydrogen phosphate (i.e., DAHP). Moreover, the untreated and aged specimen shows a decrease in the failure pressure (40–70 bar).

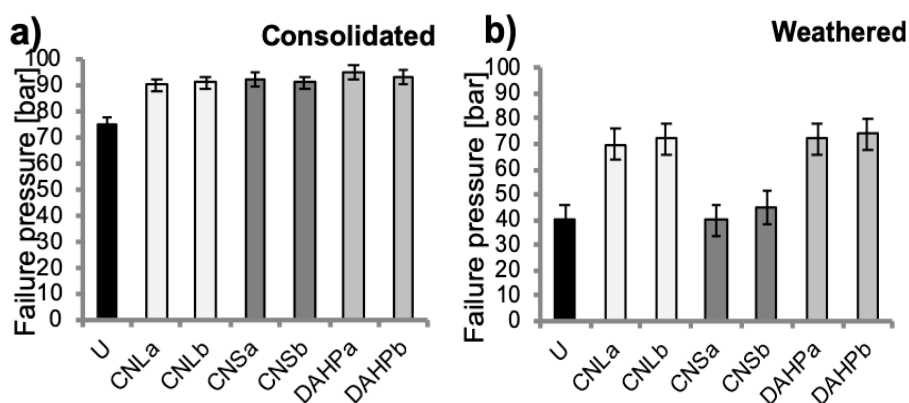


**Figure 10.** Point Load test on: (a) untreated and consolidated (unweathered) specimens; (b) untreated (weathered) and consolidated (weathered) specimens.

#### 4. Final Remarks

In this paper, the salt weathering behaviour of “Mendicino stone”, largely used in the vernacular and monumental architecture of northern Calabria, mainly in the Cosenza Province, has been assessed. Several samples, collected from a historical quarry near the city of Cosenza, were artificially weathered by salt crystallization tests. In order to evaluate the effect of consolidation on mechanical features, three different consolidating and inorganic products were then tested; respectively two commercial and another synthesized in a laboratory: (a) a suspension of nanosilica (Nano Estel<sup>®</sup>), (b) a suspension of nanolime (CaLoSiL<sup>®</sup>) and (c) a suspension of nano calcium-hydroxide mixed with diammonium hydrogen phosphate.

From colorimetric tests, all products show an absence of chromatic variation. The Scotch tape test (SST) and point load tests (PLT) suggest that all products increase the cohesive properties of the material, although the failure pressure shows a greater resistance in the samples treated with nano calcium-hydroxide mixed to diammonium hydrogen phosphate. This result is also confirmed after accelerated aging tests by salt crystallization. This increase in the properties of cohesion and mechanical strength are due to the formation of hydroxyapatite [21]. Several studies report the strengthening effectiveness of this treatment, especially on porous lithotypes [43–45].

As for the other two products tested, both those based on nanolime and nanosilica, they improved the resistance of lithotypes. However, after accelerated aging tests, a strong decrease in mechanical



strength is observable in samples treated with nanosilica. This is probably due to the poor compatibility of the nanosilica with calcareous stone samples. Better results, and almost comparable to treatments with nano calcium-hydroxide mixed to diammonium hydrogen phosphate, have been observed in the lithotypes treated with nanolime.

This research, which requires further in-depth investigation in order to understand better the features of hydroxyapatite/calcite formation, is essential for the conservation and restoration intervention of the specific cultural heritage planned within the CRATI project.

All these aspects will be carefully evaluated before elaborating the more efficient strategies of conservation and restoration intervention in situ. In fact, the use of unsuitable products, as well as the choice of inappropriate application methods during restoration works, could worsen and accelerate damage processes caused to building materials by salt crystallization.

**Author Contributions:** Methodology, S.A.R., A.M., M.L., M.M. and M.L.W.; Formal Analysis, M.R. and L.R.; Investigation, M.R. and L.R.; Data Curation, M.R.; Writing—Original Draft Preparation, M.R., L.R., N.R. and E.L.P.; Writing—Review and Editing, M.R. and L.R.; Supervision, M.F.L.R.; Project Administration, M.F.L.R.; Funding Acquisition, M.F.L.R.

**Funding:** This research is funded by the Calabria Region in the framework of the project POR CALABRIA FESR-FSE 2014-2020. ASSE I-PROMOZIONE DELLA RICERCA E DELL'INNOVAZIONE Obiettivo specifico 1.2 "Rafforzamento del sistema innovativo regionale e nazionale" Azione 1.2.2 "Supporto alla realizzazione di progetti complessi di attività di ricerca e sviluppo su poche aree tematiche di rilievo e all'applicazione di soluzioni tecnologiche funzionali alla realizzazione delle strategie di S3". CUP: J68C17000100006.

**Conflicts of Interest:** The authors declare no conflict of interest.

## References

1. La Russa, M.F.; Rovella, N.; Ruffolo, S.A.; Scarciglia, F.; Macchia, A.; Licchelli, M.; Malagodi, M.; Khalilli, F.; Randazzo, L. Consolidation of earthen building materials: A comparative study. *Archaeol. Anthropol. Sci.* **2019**. [[CrossRef](#)]
2. Ruffolo, S.A.; La Russa, M.F.; Ricca, M.; Belfiore, C.M.; Macchia, A.; Comite, V.; Pezzino, A.; Crisci, G.M. New insights on the consolidation of salt weathered limestone: The case study of Modica stone. *Bull. Eng. Geol. Environ.* **2017**, *76*, 11–20. [[CrossRef](#)]
3. La Russa, M.F.; Ruffolo, S.A.; Rovella, N.; Belfiore, C.M.; Pogliani, P.; Pelosi, C.; Andaloro, M.; Crisci, G.M. Cappadocian ignimbrite cave churches: Stone degradation and conservation strategies. *Period. Mineral.* **2014**, *83*, 187–206.
4. Lazzarini, L.; Laurenzi Tabasso, M. *Il Restauro della Pietra*; Casa Editrice Dott Antonio Milan: Padova, Italy, 1986.
5. Cultrone, G.; Sebastian, E. Laboratory simulation showing the influence of salt efflorescence on the weathering of composite building materials. *Environ. Geol.* **2008**, *56*, 729–740. [[CrossRef](#)]
6. Rodriguez-Navarro, C.; Doehne, E.; Sebastian, E. How does sodium sulfate crystallize? Implications for the decay and testing of building materials. *Cem. Concr. Res.* **2000**, *30*, 1527–1534. [[CrossRef](#)]
7. Benavente, D.; García del Cura, M.A.; Bernabéu, A.; Ordóñez, S. Quantification of salt weathering in porous stones using an experimental continuous partial immersion method. *Eng. Geol.* **2001**, *59*, 313–325. [[CrossRef](#)]
8. Flatt, R.J. Salt damage in porous materials: How high supersaturations are generated. *J. Cryst. Growth* **2002**, *242*, 435–454. [[CrossRef](#)]
9. Angeli, M.; Bigas, J.P.; Benavente, D.; Menendez, B.; Herbert, R.; David, C. Salt crystallization in pores: Quantification and estimation of damage. *Environ. Geol.* **2007**, *52*, 187–195. [[CrossRef](#)]
10. Angeli, M.; Hébert, R.; Menéndez, B.; David, C.; Bigas, J.P. Influence of temperature and salt concentration on the salt weathering of a sedimentary stone with sodium sulphate. *Geol. Soc.* **2010**, *333*, 35–42.
11. Rodolico, F. *Le pietre delle città d'Italia*, 2nd ed.; Felice Le Monnier: Firenze, Italy, 1995; pp. 427–429.
12. Bruno, E. *Scalpellini di Calabria—I Cantieri e le Scuole*; La petite Académie: Fuscaldo Marina, Italy, 1995.
13. Lico, A. Materiali Lapidei e Cave di Approvvigionamento Degli Scalpellini Roglianesi: Risorse in Calabria e Nella Provincia di Cosenza. In *La Pietra, Il Mestiere e L'arte del Decorare. Storia Della Lavorazione Della Pietra Nella Provincia di Cosenza*; Pellegrini Editore: Cosenza, Italy, 2015; pp. 74–91.

14. Milella, O. L'architettura dei Domenicani in Storia della Calabria nel Rinascimento. In *Le Arti Nella Storia*; Valtieri, S., Ed.; Gangemi: Roma, Italy, 2002; pp. 549–580.
15. Esposito, G.L. *San Domenico di Cosenza* (MD, n. s. V); Iliesi Ed.: Pistoia, Italy, 1974; p. 338.
16. Crisci, G.M.; De Francesco, A.M.; Gattuso, C.; Miriello, D. Un metodo geochimico per la determinazione della provenienza di lapidei macroscopicamente omogenei. Un esempio di applicazione sui monumenti del centro storico di Cosenza. *Arkos—Scienze e Restauro Dell'architettura* **2003**, *2*, 52–59.
17. Mastandrea, A.; Muto, F.; Neri, C.; Papazzoni, C.A.; Perri, E.; Russo, F. Deep-Water Coral Banks: An Example from the “Calcare di Mendicino” (Upper Miocene, Northern Calabria, Italy). *Facies* **2002**, *47*, 27–42. [[CrossRef](#)]
18. Critelli, S.; Le Pera, E. Geological Map of Calabria, scale 1:330,000. In *Valutazione delle Piene in Calabria. Caratteristiche Morfometriche dei Bacini della Calabria*; Gabriele, S., Ed.; Rubbettino: Soveria Mannelli, Italy, 2000.
19. Colella, A. Sedimentation, deformational events and eustasy in the perithyrranian Amantea Basin: Preliminary synthesis. *Giornale di Geologia* **1995**, *57*, 179–193.
20. Forestieri, G.; Tedesco, A.; Ponte, M.; Olivito, R.S. Local building stones used in Calabrian architecture: Calcarenite and sandstone of the Thyrrenian Coastal Range of Cosenza Province (Italy). In Proceedings of the XIV International Forum Le Vie dei Mercanti: World Heritage and Degradation, Smart Design, Planning and Technologies, Aversa/Naples/Capri, Italy, 16–18 June 2016.
21. Weththimuni, M.L.; Licchelli, M.; Malagodi, M.; Rovella, N.; La Russa, M.F. Consolidation of bio-calcarenite stone by treatment based on diammonium hydrogenphosphate and calcium hydroxide nanoparticles. *Measurement* **2018**, *127*, 396–405. [[CrossRef](#)]
22. Normal 43/93L: Misure Colorimetriche di Superfici Opache. In *Raccomandazioni Normal: Alterazioni dei Materiali Lapidari e Trattamenti Conservativi: Proposte per L'unificazione dei Metodi Sperimentali di Studio e di Controllo*; CNR: Roma, Italy; ICR: Roma, Italy, 1993.
23. Drdacky, M.; Lesák, J.; Rescic, S.; Slízková, Z.; Tiano, P.; Valach, J. Standardization of peeling test for assessing the cohesion and consolidation characteristics of historic stone surfaces. *Mater. Struct.* **2013**, *45*, 505–520. [[CrossRef](#)]
24. *Standard Test Method for Determination of the Point Load Strength Index of Rock*; ASTM D5731; ASTM International: West Conshohocken, PA, USA, 2002.
25. *Natural Stone Test Methods-Determination of Resistance to Salt Crystallization*; EN 12370; European Committee for Standardization (CEN): Brussels, Belgium, 2001; pp. 108–121.
26. Folk, R.L. Spectral Subdivision of Limestone Types. In *M 1: Classification of Carbonate Rocks—A Symposium*; Ham, W.E., Ed.; American Association of Petroleum Geologists: Tulsa, OK, USA, 1962; pp. 62–84.
27. Dunham, R.J. Classification of Carbonate Rocks According to Depositional Texture. In *M 1: Classification of Carbonate Rocks*; Ham, W.E., Ed.; American Association of Petroleum Geologists: Tulsa, OK, USA, 1962; pp. 108–121.
28. Wilson, M.J. *Clay Mineralogy: Spectroscopic and Chemical Determinative Methods*; Chapman & Hall: London, UK, 1994; pp. 11–67.
29. Comite, V.; Fermo, P. The effects of air pollution on cultural heritage: The case study of Santa Maria delle Grazie al Naviglio Grande (Milan). *EPJ Plus* **2018**, *133*, 556. [[CrossRef](#)]
30. La Russa, M.F.; Ricca, M.; Cerioni, A.; Chilos, M.G.; Comite, V.; De Santis, M.; Rovella, N.; Ruffolo, S.A. The colors of the Fontana di Trevi: An analytical approach. *Int. J. Archit. Herit.* **2018**, *12*, 114–124. [[CrossRef](#)]
31. La Russa, M.F.; Comite, V.; Aly, N.; Barca, D.; Fermo, P.; Rovella, N.; Antonelli, F.; Tesser, E.; Aquino, M.; Ruffolo, S.A. Black crusts on Venetian built heritage, investigation on the impact of pollution sources on their composition. *EPJ Plus* **2018**, *133*, 370. [[CrossRef](#)]
32. Barca, D.; Comite, V.; Belfiore, C.M.; Bonazza, A.; La Russa, M.F.; Ruffolo, S.A.; Crisci, G.M.; Pezzino, A.; Sabbioni, C. Impact of air pollution in deterioration of carbonate building materials in Italian urban environments. *Appl. Geochem.* **2014**, *48*, 122–131. [[CrossRef](#)]
33. La Russa, M.F.; Ruffolo, S.A.; Belfiore, C.M.; Aloise, P.; Randazzo, L.; Rovella, N.; Pezzino, A.; Montana, G. Study of the effects of salt crystallization on degradation of limestone rocks. *Period Miner.* **2013**, *82*, 113–127.
34. Brimblecombe, P.; Grossi, C.M. Aesthetic thresholds and blackening of stone buildings. *Sci. Total Environ.* **2005**, *349*, 175–189. [[CrossRef](#)]
35. Rampazzi, L.; Andreotti, A.; Bonaduce, I.; Colombini, M.P.; Colombo, C.; Toniolo, L. Analytical investigation of calcium oxalate films on marble monuments. *Talanta* **2005**, *63*, 966–977. [[CrossRef](#)]

36. Sabbioni, C.; Zappia, G. Oxalate patinas on ancient monument: the biological hypothesis. *Aerobiologia* **1991**, *7*, 31–37. [[CrossRef](#)]
37. UNI 10921:2001 *Beni Culturali—Materiali Lapidei Naturali ed Artificiali—Prodotti Idrorepellenti—Applicazione su Provini e Determinazione in Laboratorio delle Loro Caratteristiche*; UNI: Milano, Italy, 2001.
38. Witzel, R.F.; Burnham, R.W.; Onley, J.W. Threshold and suprathreshold perceptual color differences. *JOSA* **1973**, *63*, 615–625. [[CrossRef](#)]
39. La Russa, M.F.; Ruffolo, S.A.; Álvarez de Buergo, M.; Ricca, M.; Belfiore, C.M.; Pezzino, A.; Crisci, G.M. The behaviour of consolidated Neapolitan yellow Tuff against salt weathering. *Bull. Eng. Geol. Environ.* **2017**, *76*, 115–124. [[CrossRef](#)]
40. Benavente, D.; Martinez Martinez, J.; Cueto, N.; Garcia del Cura, M.A. Salt weathering in dual-porosity building dolostones. *Eng. Geol.* **2007**, *94*, 215–226. [[CrossRef](#)]
41. Evans, I.S. Salt crystallization and rock weathering: A review. *Revue de Geomorphologie Dynamique* **1970**, *19*, 153–177.
42. Benavente, D.; Garcia del Cura, M.A.; Fort, R.; Ordonez, S. Durability estimation of porous building stones from pore structure and strength. *Eng. Geol.* **2004**, *74*, 113–127. [[CrossRef](#)]
43. Benavente, D.; Garcia del Cura, M.A.; Ordonez, S. Salt influence on evaporation from porous building rocks. *Construct. Build. Mater.* **2003**, *17*, 113–122. [[CrossRef](#)]
44. Yang, F.; Liu, Y.; Zhu, Y.; Long, S.; Zuo, G.; Wang, C.; Guo, F.; Zhang, B.; Jiang, S. Conservation of weathered historic sandstone with biomimetic apatite. *Chin. Sci. Bull.* **2012**, *57*, 2171–2176. [[CrossRef](#)]
45. Yang, F.; Zhang, B.; Liu, Y.; Wei, G.; Zhang, H.; Chen, W.; Xu, Z. Biomimic conservation of weathered calcareous stones by apatite. *New J. Chem.* **2011**, *35*, 887–892. [[CrossRef](#)]



© 2019 by the authors. Licensee MDPI, Basel, Switzerland. This article is an open access article distributed under the terms and conditions of the Creative Commons Attribution (CC BY) license (<http://creativecommons.org/licenses/by/4.0/>).